International Journal of Veterinary Science

www.ijvets.com P-ISSN: 2304-3075 E-ISSN: 2305-4360 editor@ijvets.com

RESEARCH ARTICLE

Morphological Analysis of the Tibia from the African Ostrich

Lei Wang[1], Kemei Peng[1], Jiayue Cheng, Min Chen, Chunyan Jin, Tingting Liu and Weiwei Ca

College of Animal Science and Veterinary Medicine, Huazhong Agricultural University, Wuhan, P. R., China 430070; [1]Department of Anatomy, Histology and Embryology, College of Animal Science and Veterinary Medicine, Huazhong Agricultural University, Wuhan 430070, People's Republic of China

ARTICLE INFO

Received: January 16, 2013
Revised: March 15, 2013
Accepted: March 16, 2013

Key words:
Bone mineral density (BMD)
Osteons
Resorption pits
Transition area

***Corresponding Author**
Kemei Peng
kmpeng1010@126.com

ABSTRACT

The Ostrich tibia belongs to the long bone, which has a complex structure comprising to different types of bone cell, a calcified extracellular matrix and two crisscross pipelines. Few present report concerning on the histological structure of Ostrich tibia had been carried out. This experiment was carried out to investigate the Tibia Morphological characteristics of four Ostriches (one-year-old) with Bone mineral density (BMD), ultrastructure (SEM) and microstructure. The results indicated the BMD of the Ostrich tibia was high, 7-fold greater than chicken (breeding birds) and scanning electron microscopy showed firm and strong, without any honeycomb-shaped structure. Microstructure had three characteristics: layers of cortical bone are clear; outer circumferential lamella and inner circumferential lamella are thicker than those in other animals; a special "transition zone" between the outer circumferential lamella and osteon zone is present. In addition, degeneration and coalesces together with tibia gradually.

Cite This Article as: Wang L, K Peng, J Cheng, M Chen, C Jin, T Liu and W Ca, 2013. Morphological analysis of the tibia from the African Ostrich. Inter J Vet Sci, 2(2): 39-43. www.ijvets.com

INTRODUCTION

The Ostrich, *Struthio camelus*, is classified within the kingdom Animalia, Aves, Paleognathae, Struthioniformes order of ratites. *Struthio camelus* is the only living species of its genus, *Struthio*. The Ostrich is thus an interesting subject concerning animal evolution and Morphology studies. The Ostrich has long muscular legs with a skeleton that is similar to other birds in terms of structure and appearance but highly distinctive with respect to the amazing running speeds of these birds and non-ability to fly. It has thus been speculated that Ostrich legs would have distinct tissue structures and physiological function but this has not been previously studied in detail. The aim was to describe the morphology of the tibial cortical bone of the African Ostrich. The objective of this study was to investigate the Tibia Morphological characteristics of four Ostriches (one-year-old), which may provide valuable data for future comparative anatomical and evolutionary studies and also provide a theoretical basis for novel Ostrich breeding management and disease prevention strategies.

MATERIALS AND METHODS

Animals

Two female and two male healthy, one-year-old African Ostriches were obtained from the Zhengzhou Jinlu Ostrich Farm in Henan province. The birds were deeply anesthetized with 15% urethane (Caoyang Secondary Chemaical Plant, Shanghai, China) at a dose of 1.2 g/kg body weight, and bloodletting from arteria cervicalis to death. The tibia was exposed completely, and measured length and weight of tibia. Then Bone mineral density (BMD) of proximal tibia was measured using Dual-Energy X-Ray Absorptiometry (Lunar PIXImus2 densitometer, General Electric Medical Systems, USA) immediately.

Tissue preparation for electronic microscope observation

$3\times3\times3mm^3$ bone blocks were cut off from 1/4 closed to proximal of each tibia, fixed in 2% paraformaldehyde-2.5% glutaraldehyde solution for 2 hours in 4°C freezer. And the blocks were washed using sodium cacodylate solution (pH 7.2) for 30min. Then bone blocks were fixed in 1% osmic acid for 2 hours in 4°C freezer, and washed by ultrapure water for 30min. After all the treatment

including dehydration, replacement by isoamyl acetate, critical point drying and plating film of gold, the bone blocks were observed the ultrastructure of the inside surfaces of the bones from the tibia necks using scanning electron microscopy (Quanta 200, FEI Company, Holland).

Tissue Preparation for Ground Slices

0.5cm-thick discuses were sawn off at the 1/4 closed to proximal of each tibia to observe the layers on the cross-section of tibia by naked eyes. And then, the bone blocks were fixed for 72 hours with 4% neutral paraformaldehyde. Then, these bone pies were divided into three groups. Bone blocks in Group 1 were polished into slices about 20μm thick on holystone manually. The next process included dehydration using gradient alcohol (1h/step), immersion in ethylether for 30min, atmospheric drying, immersion in xylene for 30min, mounting with neutral gummi, and drying for 48 hours. The ground slices were observed under light microscope for microstructure. The blocks in Group 2 were made into 20μm-thick slices as Group 1. After dehydration from 75%-95%, the slices were stained by 1% crystal violet (95% alcohol) solution for 36 hours. And as Group 1, after immersion in 95% and 100% alcohol, ethylether, drying, the slices were continues to be ground thinner about 12-15μm-thick in xylene solution. Then the slices could be observed under light microscope after mounting and atmospheric drying.

Tissue Preparation for Paraffin Slices

Bone discuses in Group 3 were treated in neutral 13% EDTA at 4°C for decalcification. Put the beaker with 4°C EDTA and bone discuses into another bigger beaker with ice water, and put both of them in microwave on 250W output. It is important to make sure the temperature of EDTA solution is lower than 15°C by changing the ice water in the bigger beaker frequently. About 3 hours later, the bone discuses turned a little softer. Cut them into $1\times1\times0.5cm^3$ blocks, and went on treated in microwave. After 15 hours, the bone blocks were enough soft and they could be cut easily without any barrier. After groovy dehydration, clearing and waxdip, samples were embedded in paraffin and 9μm sections were cut and stained with hematoxylin and eosin (H&E) and viewed with a bright field microscope. Photomicrographs (IX71, Olympus, Japan) were taken to observe and record the morphology.

RESULTS

The results obtained from this experiment confirm that the BMD of Ostriches bone was high, and the structure of bone especially tibia was stronge. Tibias from Ostriches were about 51 cm long and 32 kg in weight, and showed a very high BMD ranging from 3.436 g/cm^2 to 8.677 g/cm^2 (average 5.656 g/cm^2) and a T-score ranging from 37.0 to 102.5 (average 62.0) (Fig. 1a, 1b). It was striking that different portions of the tibia had such different values (Fig. 1c). The proximal tibia had a slightly lower BMD of 5.6 g/cm^2 on average which is similar to that of the distal ending. The BMD of the tibia diaphysis was a little higher at about 6.2 g/cm^2.

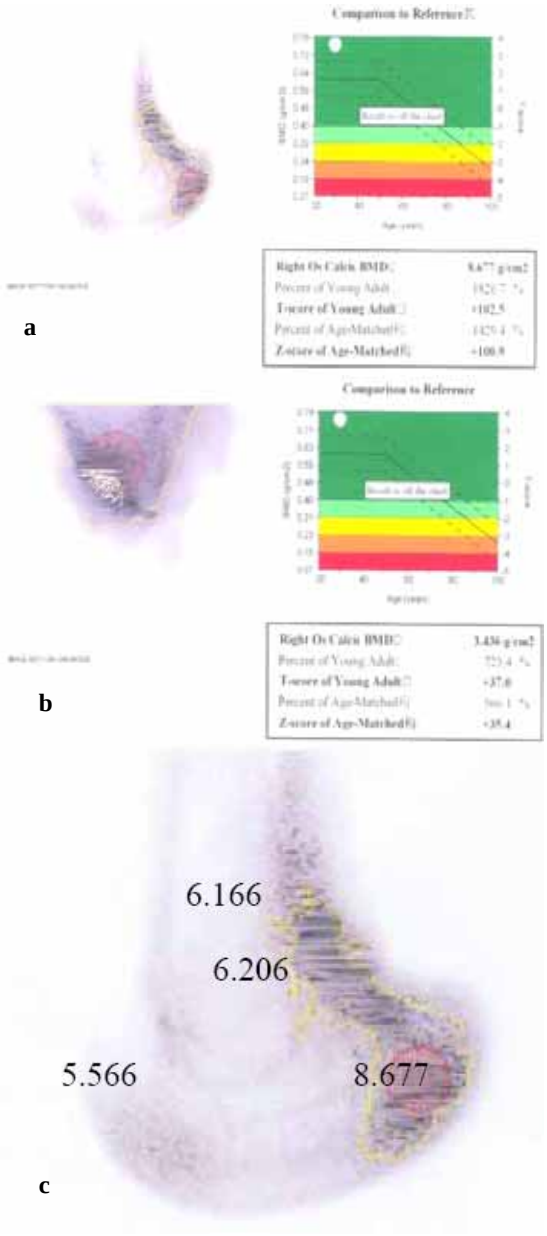

Fig. 1a: The report of tibia with lowest BMD value. **b)**. The report of the part in tibia with highest BMD value. **c)**. Different part in Ostrich tibia with different BMD value.

There was little spongy bone detected in the one-year-old Ostrich tibia diaphyses under the scanning electron microscopy. Two Haversian canals were observed but there were no fibers covering the wall of the central canal, although a bone canaliculus lacuna was evident (Fig. 2a). Many resorption pits were revealed on the bone surface, which may indicate the beginning or finishing period of resorption (Fig. 2b). Mineralized collagen fibers covered the surface facing the marrow, and they maybe composed to the net-shape new born bone (Fig. 2c, d). On the smooth surface, some resorption and reconstruction trails could be seen and with some granular new bone tissues on (Fig. 2e, f).

The microstructure of tibia is complex; tibia compact bone is divided into five ribbons: outer periosteum, outer circumferential lamella, transition area, osteon zone, and

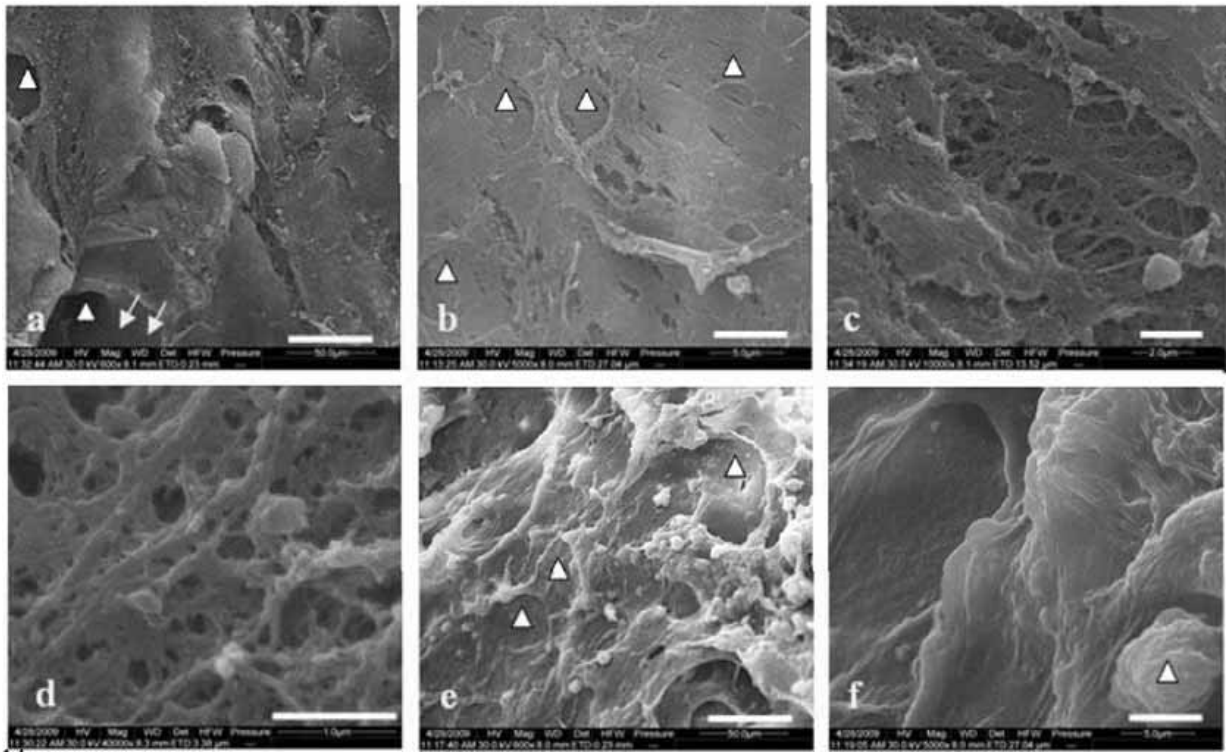

Fig. 2a: Triangles signed Haversian canals, with arrows signed bone canaliculus lacuna on it. Bar=50µm. **b)** Triangles signed Resorption pits on bone surface. Bar=5µm. **c)** Mineralized collagen fibers cover on the bone surface. Bar=2µm. **d)** Net-shape new bone. Bar=1µm. **e)** Triangles signed Resorption trails on smooth bone surface. Bar=50µm. **f)** Triangle signed granular new bone. Bar=5µm.

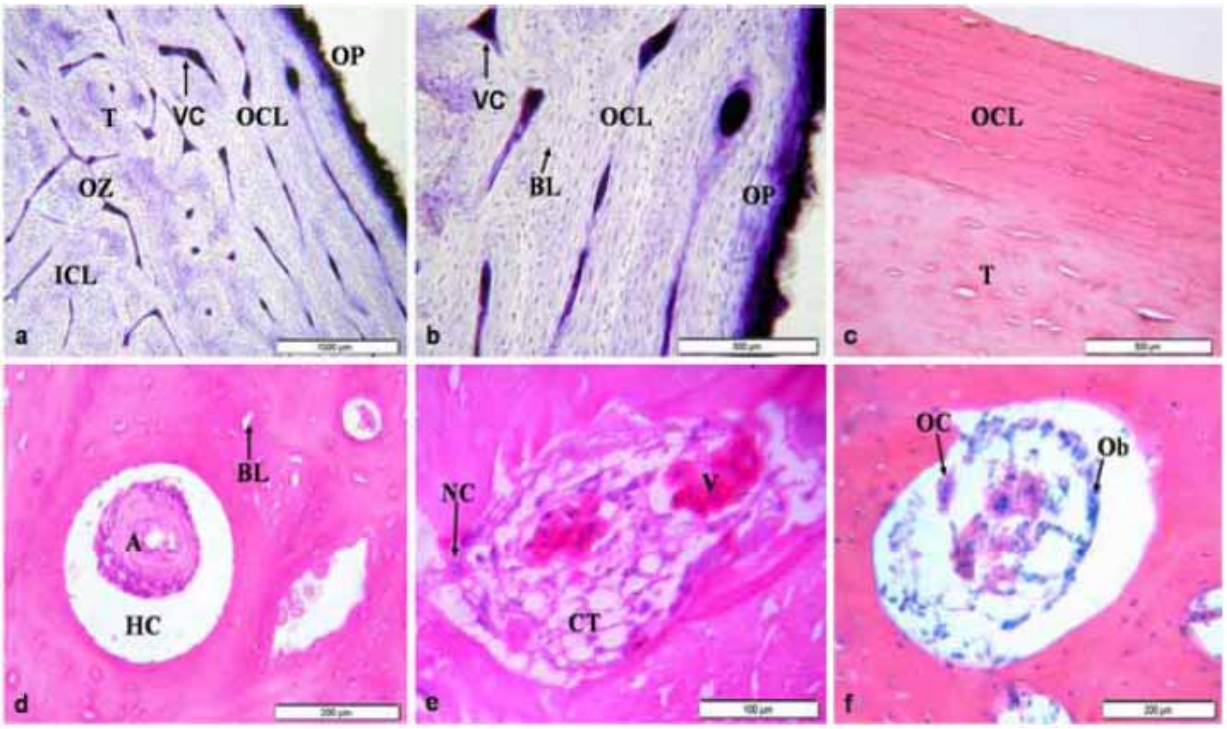

Fig. 3a: Microspecimen stained by crystal violet showed outer periosteum (OP), outer circumferential lamella (OCL), the deeper stained transition area (T), zone of osteon (OZ), and Inner circumferential lamella (ICL). Bar=1000µm. **b)** Microspecimen stained by crystal violet showed Volkman`s canal (VC). Bar=500µm. **c)** The transition area (T) is lighter stained than OCL. (HE stained slice) Bar=1000µm. **d)** An arteriole (A) in Haversian canal (HC), and bone lacuna (BL). (HE stained slice) Bar=200µm. **e)** Venula (V), surrounding connevtive tissue (CT), and a nerve cell (NC). (HE stained slice) Bar=100µm. **f)** Osteoblasts (Ob) and osteoclasts (Oc). (HE stained slice) Bar=200µm.

inner circumferential lamella (Fig. 3a). The tibia is covered by an outer periosteum (Fig. 3b) composed of dense connective tissue, which divided into an outer fiber layer and an inner layer. The inner layer harbors more cells than the fiber layer and contains both collagen fiber and osteoblasts. The outer circumferential lamella comprising many small lacunae containing osteocytes and small perforating tubes, bone lacunae were found to be arranged along the direction of the bone lamella and to be small and fusiform in shape (Fig. 3c). The Volkmann's canal stained strongly with crystal violet the Volkmann's canal, crossing perpendicular to the lamella in a net-shape (Fig. 3c), but is colorless when stained using HE method (Fig. 3d). Additionally, many layers of concentric lamellae and arranged closely and in parallel with the surface of the bone (Fig. 3d).

A novel structure called "transition area" was located between the outer circumferential lamella and the osteon area. In this region, the arrangement of bone lamellae was altered from surrounding the marrow in parallel with the surface of bone into independent units that gradually surround their own central Haversian canal. It showed much deeper crystal violet staining than the outer circumferential lamella or the inward area of the osteon (Fig. 3b), but was lighter in color on HE stained slices (Fig. 3d).

The osteon area is composed of osteons and interstitial lamellae. An osteon is cylindrical in shape and consists of a central hole, the Haversian canal through which blood vessels run (Fig. 3e). A lacunar system is also evident and is arranged in a crisscross pattern between the neighboring central canals of the osteons, the Volkmann's canal, and blood vessels and nerve fibers pervade this area (Fig. 3e). The Volkmann's canals and central canals together provide blood to the bone. The interstitial lamella is located among neighboring osteons and is irregularly shaped with no central canal. This interstitial lamella represents the remainder of older absorbed osteons and the circumferential lamella.

Metrocytes, osteoblasts, multinucleated osteoclasts, and a large number of osteocytes were obversed in tibia. Osteoblasts are smaller and thinner than osteoclasts, and have a short bar shaped or flat morphology with an elliptical nucleus and basophilic cytoplasm arranged in rows at the surface of the new bone flap (Fig. 3f). The larger osteoclasts contain one or more nuclei and acidophilic cytoplasm, and are distributed within the bone reabsoption or remodeling tissue and surrounded by osteoblasts and connective tissue (Fig. 3f).

DISCUSSION AND CONCLUSION

The present results lead to conclude that mechanical strength also noticeably weakened with a decrease in BMD, and the organic and inorganic matter contents were much reduced, most prominently in the case of inorganic matter, which indicates that the BMD is proportional to the levels of inorganic matter, principally hydroxyapatite affecting the bone strength and the most convenient and commonly indicator of evaluating the bone strength. The BMD values of ostrich tibia was truly surprising as they measured 4-8 times the corresponding values in human and 7-fold greater than chicken (breeding birds). The high BMD is an important reason for the anatomy and functional characteristics of the Ostrich long and slim legs, and high running capability in desert terrains. The BMD of the Ostrich tibia shaft was found to be more uniform and higher on average than other regions of this bone. For a young Ostrich, we found that the proximal tibia is almost completely composed of hard solid bone with little epiphysis but has maybe the lowest BMD. Above all, the lowest BMD of the Ostrich tibia is still much higher than human. And it was interesting that different portions of the proximal tibia had such different values, which is not found in human bone.

The structure of the Ostrich tibia was found to be unlike that of other birds, but similar to the mammalian tibia. Compared with cat, the compact bone of the Ostrich tibia is very thick and has clearly defined layers. The cement line of the osteon in Ostrich tibia is also more clearly observable under the light microscope. In this regard, it is hard to discern the outer circumferential lamella of the cat tibia, whilst in the Ostrich tibia a thick layer of outer circumferential lamella that has a protective role by surrounding the outer areas is readily detectable. In addition, a thick layer of inner circumferential lamella is found in the Ostrich tibia whereas this is not evident in chickens or humans.

In the research, a novel region appears to be specific to the Ostrich and denoted the "transition area". No such region has to our knowledge been previously reported. This area is visible to the naked eyes and stains strongly with crystal violet but only weakly by HE method. The outer circumferential lamellae of the transition area show an altered arrangement, from the typical wall-shape to independent units that form along the tibial surface to surround the Haversian canal. It appears that the new osteons arise from this region, and we speculate that the absorption and reconstruction of bone is likely to be very active here also.

Lots of granular new bone and mineralized collagen fibers cover on the bone surface under the scanning electron microscope, the Ostrich tibia appears to be much stronger and more active than that of either rat or human. The further attempted to compare the ultrastructure of the Ostrich tibia with dinosaur bone using the electron microscope, but could not draw any significant conclusions. Ultrastructure information for the transition area was also not possible to acquire at this stage due to the high BMD of the Ostrich bone which prevented us from generating $1mm^3$ blocks in this precise location. Overcoming this technical limitation will require the development of new methodologies in the future.

Acknowledgement

Grant support: Natural Science Foundation of China No.30471249 and No. 30972152, and Specialized Research Fund for the Doctoral Program of China Higher Education No. 200805040023. We thanks for the help of Zhengzhou Jinlu Ostrich Farm in Henan province.

REFERENCES

Armitage M, 2001. Scanning Electron Microscope Study of Mummified Collagen Fibers in Fossil Tyrannosaurus Rex Bone. Creation Research Society Quarterly, 38: 61-66.

Chen YX, 2007. Bone, in: Bacha W. J. and Bacha L. M. (editors), Color Atlas of Veterinary Histology, China Agricultural University Press, Beijing, pp: 21-26.

Cheng JY, KM Peng, EH Jin, Y Zhang, Y Liu, NB Zhang, H Song, HZ Liu and ZL Tang, 2011. Effect of Additional Boron on Tibias of African Ostrich Chicks. Biol Trace Elem Res, 144: 538-549.

Gartner LP and Hiatt JL, 2008. Bone, in: Color Atlas of Histology, Chemical Industry Press, Beijing, pp: 37-41.

Li XG and HZ Jiang, 1999. The whole skeleton characteristics of Ostrich. Journal of Jilin Agricultural University, 21: 86-88.

Linnaeus C, 1758. S. pedibus didactylis, in: Systema Naturae (Systema naturae per regna tria naturae, secundum classes, ordines, genera, species, cum characteribus, differentiis, synonymis, locis. TomusI. Editio decima, reformata), Holmiae, Stockholm, pp: 155.

Yang JH, RL Wang, Y Cao, YR Fei, YY Huang, W He and J Liu, 2009. Evaluation of anti-osteoporosis in ovariectomized Wistar rats treated with antler blood by synchrotron radiation X-ray fluorescence microprobe. Spectroscopy: An Inter J, 1: 1-9.

Ma T, 2007. Influence of Jump on rat bone morphometry and biomechanics indicator. Master Dissertation (East China normal university, The College of physical education and health, 13-27.

Shen Y, LY Dai, ZM Zhang, SD Jiang and LS Jiang, 2009. Postmenopausal women with osteoarthritis and osteoporosis show different ultrastructural characteristics of trabecular bone of the femoral head. BMC Musculoskeletal Disorders, 10: 35.

Vazquez E, L Song and B Dawson, 2004. Precision of Bone Mineral Density Scans at the Proximal Tibia. Journal Clinical Densitometry, 7: 222.

Qin LP, QY Zhang, YP Tian, HC Zheng, M Huang and BK Huang, 2003. Total coumarins from fruitsof Cnidium monnieri inhibit formation and differentiationof multinucleated osteoclasts of rats Acta Pharmacol Sin, 24: 181-186.

Wang SY, HQ Li, XQ Yang, P Zhai and J Zhu, 1999. Bone growth disorder in vitamin D deficient, calcium deficient elder chicken. Journal of Chongqing Medical University, 24: 142-145.